Plasma molding over surface topography: Energy and angular distribution of ions extracted out of large holes

Chang-Koo Kim and Demetre J. Economou[a)]
Plasma Processing Laboratory, Department of Chemical Engineering, University of Houston, Houston, Texas 77204-4004

(Received 8 May 2001; accepted for publication 19 November 2001)

Plasma molding over surface topography was investigated by measuring the energy and angular distribution of ions extracted from a hole in contact with a high density plasma. Holes with diameter larger than as well as smaller than the local sheath thickness were studied in argon or deuterium gas. When the hole diameter (10 μm) was much less than the sheath thickness, the plasma was not perturbed by the presence of the hole. The ion energy distribution (IED) had multiple peaks due to ions sampling the time-varying potential while crossing the sheath. The ion angular distribution (IAD) was Gaussian, peaking at zero angle with respect to the surface normal. These results agree with reported studies. At the other extreme, when the hole diameter (1270 μm) was larger than the sheath thickness, plasma "leaked" into the hole. The IED had a single peak since ions now experience an average sheath potential. The IAD was quite broad extending beyond 30° off normal. When the hole diameter (508 μm) was comparable to the sheath thickness, the shape of the IED and IAD was in-between the two extremes mentioned above. The IAD became more isotropic with increasing power, suggesting that the plasma leaked only partly through the hole (the plasma–sheath meniscus was located inside the hole). For all cases, increasing pressure resulted in lower ion energy in argon plasmas due to ion–neutral collisions. Increasing pressure had little effect on the ion energy for deuterium plasmas, for hole diameter less than 508 μm. This is due to the smaller ion–neutral collision cross section for deuterium. © *2002 American Institute of Physics.*
[DOI: 10.1063/1.1435423]

I. INTRODUCTION

The ability of plasma to mold around surfaces of complex shape finds application in coating of curved objects, etching of surfaces of complex form (e.g., for MEMS), plasma immersion ion implantation, and ion extraction from a plasma by electrically biased grids (for use in ion beam assisted growth and etching of thin films, neutral beam etching, ion thrusters, neutron generators, etc).[1,2] The interaction of a plasma with a surface containing topographical features is critical to all of these applications. The flux, energy, and angular distributions of ions incident on the target are of primary importance. These quantities depend critically on the shape of the meniscus (plasma–sheath boundary) formed over the surface topography.

For plasma–grid interaction, the important length scales that control behavior are the plasma sheath thickness l and the diameter of the grid holes d. The sheath thickness is related to the Debye length λ_D. When the surface is floating, the sheath is a few λ_D thick. On the other hand, when the surface is biased negatively to extract positive ions, the sheath thickness increases to several tens of λ_D, depending on the magnitude of the applied voltage.

Figure 1 shows three cases of plasma molding over holes. In Fig. 1(a) (top), l is much larger than d so that the presence of holes does not disturb the plasma. The plasma–sheath boundary remains nearly planar as if the hole were a solid wall. In Fig. 1(b) (middle), l is much smaller than d so that the plasma–sheath interface follows the surface contour. Plasma leaks through and under the holes. Figure 1(c) (bottom) is an intermediate situation where l is comparable to d and there is significant disturbance of the plasma–sheath boundary due to the presence of the holes.

Figures 1(a)–1(c) will produce different angular distributions of ions extracted from the plasma. Case (a) will result in a rather collimated ion beam (assuming no ion collisions in the sheath), while cases (b) and (c) will produce a divergent beam. Varying the hole axial thickness can also control the beam divergence. Thicker holes should produce less divergent beams, since the diverged ions will strike the sidewalls and neutralize. Finally, the ion energy can be controlled by the magnitude of the potential of the sheath over the hole. The required ion beam quality (energy and divergence) depends on the application. For example, neutral beam sources for anisotropic etching applications require a collimated beam, while coating the sidewalls of microscopic features in ion beam assisted deposition or surface cleaning of sidewalls is facilitated with divergent beams.

In this study, an experimental system and a methodology were developed to investigate the interaction of a plasma with a single hole. This was thought to be a well-defined experiment to study plasma–grid interaction. Holes were selected so that the hole diameter was less than, larger than, and comparable to the sheath thickness. Holes with the same diameter, but with different thickness as were also used to

[a)]Author to whom correspondence should be addressed; electronic mail: economou@uh.edu

 © 2002 American Institute of Physics

Downloaded 31 May 2002 to 129.7.12.23. Redistribution subject to AIP license or copyright, see http://ojps.aip.org/japo/japcr.jsp

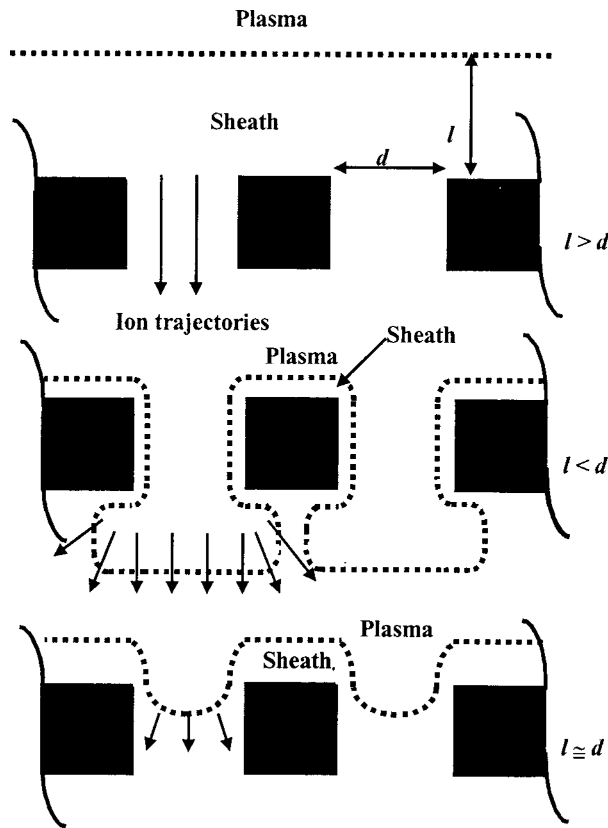

FIG. 1. Schematic of plasma molding over holes: (a) sheath thickness l is larger than hole diameter d; (b) l is smaller than d; and (c) l is comparable to d.

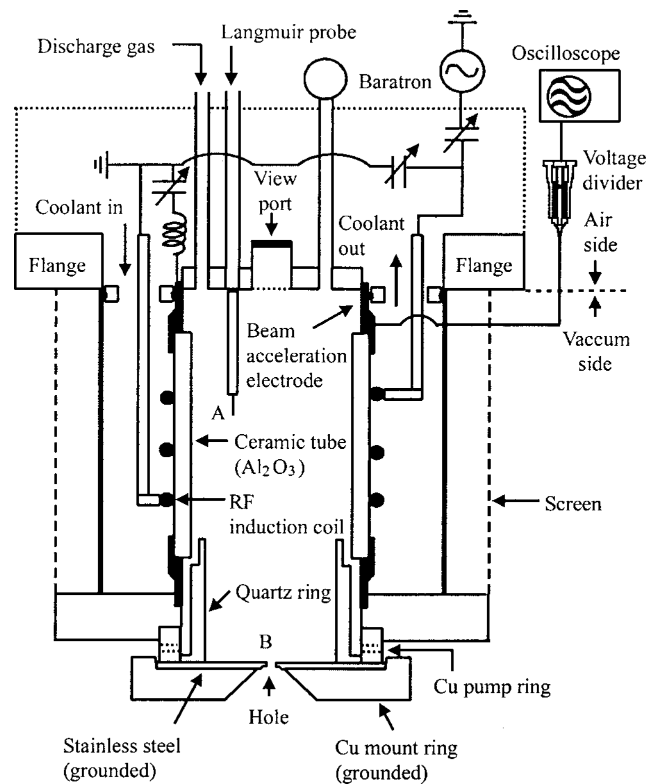

FIG. 2. Schematic of the rf inductively coupled plasma source. Point A is where a Langmuir probe was located to measure bulk plasma parameters. Point B is where the sheath is formed over the hole.

investigate the effect of the hole aspect ratio. Experiments were conducted in both argon and deuterium plasmas.

Measurements of the energy and angular distributions of ions extracted from a plasma through a hole that intentionally perturbs the plasma (a hole with diameter greater than the sheath thickness) have not been reported.

II. EXPERIMENT

A. Plasma source

An inductively coupled high-density plasma (Fig. 2) was used based on an earlier design by Chen.[2] The gas being discharged (argon or deuterium) was introduced from the top and was regulated using a mass flow controller (Unit Instruments, UFC-1400A). The pressure in the plasma source was monitored by a capacitance manometer (MKS, Baratron 622 A), and was varied from 5 to 50 mTorr for argon and 10 to 50 mTorr for deuterium. A radio frequency (rf) circuit and a matching network were attached to the air side of the 6 in. ConFlat™ flange holding the source. The plasma was ignited in a ceramic tube (Al_2O_3) 1.25 in. in inner diameter and 3.25 in. in length, by applying 13.56 MHz rf power (ENI Power Systems, OEM-6AM-1-B) to a three-turn coil through the matching network. The matching network consisted of two variable capacitors (5–500 pF) connected to the rf power supply in series and parallel, respectively. The induction coil was cooled by de-ionized water at $\sim 19\,°C$, circulated by a chiller (Neslab Instruments Inc., HX-200), to prevent overheating of the coil. A 0.5 in. diam sapphire window on the top of the plasma source allowed visual inspection of the plasma.

Ions could be accelerated by a beam acceleration electrode (aluminum) attached to the top portion of the plasma source. The plasma potential could be controlled by a variable air capacitor connected to the beam acceleration electrode through an inductor. This boundary-driven plasma potential has been used for producing neutralized plasma beams.[2,3] A high voltage divider probe (Tektronix) was used to measure the voltage on the beam acceleration electrode (called "boundary voltage" hereafter). The peak value of the boundary voltage could be varied from -250 to $+150$ V with respect to ground. During the experiments reported herein, the boundary voltage was set to its minimum value (less than ± 10 V) at each power and pressure condition.

A copper pump ring with six slits (to allow gas flow) was attached to the bottom of the plasma source. A copper mounting ring was attached to this pump ring to hold in place a grounded stainless steel plate with a hole and the ion analyzer. The source was equipped with a Langmuir probe to measure bulk plasma parameters such as plasma density and electron temperature.

The plasma source was mounted on an ultrahigh vacuum (UHV) chamber with a 6 in. ConFlat™ flange. The UHV chamber was pumped by a 300 l/s turbomolecular pump (Alcatel, 5401CP), backed by a two-stage rotary mechanical pump (Edwards, E2M40). The pressures in the UHV chamber and in the foreline were measured by a nude ionization gauge (Granville–Phillips, BA type) and a thermocouple

Downloaded 31 May 2002 to 129.7.12.23. Redistribution subject to AIP license or copyright, see http://ojps.aip.org/japo/japcr.jsp

gauge (Granville-Phillips, 27006), respectively, and were monitored on a vacuum gauge controller (Granville-Phillips, 307). During experiments (with gas flowing into the plasma source), a pressure of about 1×10^{-5} Torr was routinely achieved in the UHV chamber.

The experimental strategy was as follows:

(1) measure the plasma density and electron temperature by the Langmuir probe to estimate the sheath thickness,
(2) choose the hole diameter based on the sheath thickness, and
(3) measure the flux, energy and angular distributions of ions for the cases where the hole diameter is much less than, comparable to, and larger than the sheath thickness, and for different hole aspect ratios.

Several different holes were used. A 10 μm diam hole was made by laser drilling of a 2.5 μm thick nickel foil attached on the stainless steel plate (National Aperture, Inc.). 508 μm and 1270 μm diam holes were directly drilled on a 254 μm thick stainless steel plate (Spectralytics). These holes represent cases where the hole diameter is much smaller than the sheath thickness (10 μm), larger than the sheath thickness (1270 μm), or comparable to the sheath thickness (508 μm). Experiments were also conducted with holes having the same diameter of 127 μm, but with different thickness, namely 25.4 and 254 μm.

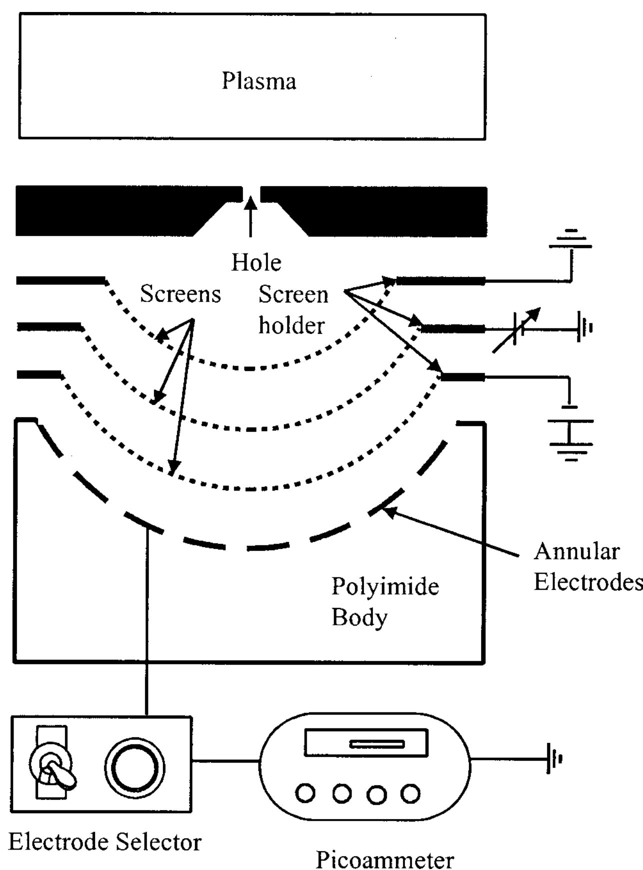

FIG. 3. Schematic of the ion analyzer for measuring energy and angular distributions of ions. The collecting electrodes and the screens were sections of concentric hemispheres having their center at the hole.

B. Ion analyzer

A gridded retarding field ion analyzer[4–9] was used to measured both the energy and angular distributions of ions striking the grounded electrode (Fig. 3). The analyzer was almost identical to that used at Sandia National Laboratory,[4–7] with small modifications for our purpose. The analyzer consisted of three screens and 11 annular current collecting electrodes. All screens and collecting electrodes were shaped as part of concentric hemispheres centered at the hole. The collecting electrodes were electrically isolated by epoxy, so that each electrode was 2°–3° wide. The hemispherical screens were mounted on stainless steel screen holders by holding the screens between a hemispherical brass mandrel and the screen holders, and spot welding them following Taylor.[10] The top screen (closest to the hole) and the bottom screen (closest to the collecting electrodes) were 50 wires/in. (90% transparency) with 0.001 in. wire diameter and 0.019 in. square openings. The middle screen was 100 wires/in. (81% transparency) with 0.001 in. wire diameter and 0.009 in. square openings. All screens were made of stainless steel (Unique Wire Weaving Co, Inc.). The ion analyzer assembly produced a distance of 1.1 in. from the hole to the collecting electrodes. The top screen was grounded to create a field-free region between the hole and the ion analyzer to preserve the ion path after ions penetrated through the hole. The bottom screen was biased at −90 V to repel electrons from the plasma and also repel secondary electrons emitted from the collecting electrodes.

To obtain the ion energy distributions, the middle screen was swept from 0 (ground) to positive voltages at intervals of 1 V until the measured current was zero. Only ions with energies greater than the middle screen potential would pass through the screen and be detected by the collecting electrodes. Five current measurements were taken at each voltage on the middle screen and averaged to obtain each data point. The ion energy distribution function was obtained by differentiating the current at the collecting electrodes with respect to voltage on the middle screen. The current at zero voltage to the middle screen allows one to measure the total ion flux. The total ion flux was obtained by dividing the total current by the hole area after the transmissions of the screens were accounted for, i.e., the measured current was divided by $0.9\times0.9\times0.81$.

Assuming perfectly flat screens, the energy resolution ($\Delta E/E$) of an ion analyzer is limited by the finite hole size of the middle screen and the distance between the middle screen and the adjacent screens. Sakai and Katsumata[11] studied the influence of geometrical factors on the energy resolution of a retarding field electrostatic analyzer made of three screens. Based on their results and the geometrical parameters of the ion analyzer used in this work, the energy resolution was estimated to be about 3%–4%.

To obtain the ion angular distributions, the middle screen was set to 0 V to allow all ions to reach the collecting electrodes. An ion will hit one of the collecting electrodes according to its angle coming out of the hole. Thus, measurement of the ion current at each collecting electrode gave the ion angular distribution. Five current measurements were

Downloaded 31 May 2002 to 129.7.12.23. Redistribution subject to AIP license or copyright, see http://ojps.aip.org/japo/japcr.jsp

taken at each electrode and averaged to obtain each data point.

Due to the finite thickness of the hole, an ion incident normal to the hole plane "sees" a greater opening than an ion approaching at an off normal angle. This effect was corrected following Liu *et al.*[12] The correction was applied for the 10 μm diam hole only, since the work of Liu *et al.* assumes that the plasma–sheath boundary remains planar (no plasma disturbance).

Voltages on the bottom and the middle screen were applied by HP (6209) and Kepco (BHK 500-0.4MG) dc power supplies, respectively. Currents at the collecting electrodes were measured by a picoammeter (Keithley, 485). The dc power supplies and the picoammeter were controlled by a National Instruments PCI general purpose interface bus (GPIB) using LABVIEW 5.1 for Windows.

III. RESULTS AND DISCUSSION

A. Sheath thickness versus hole diameter

Experiments were conducted over the pressure range of 5–50 mTorr and 10–50 mTorr for argon and deuterium plasmas, respectively. The power range was 200–600 W for both plasmas. The reported power is a nominal value and not necessarily the true power dissipated in the plasma, i.e., power losses in the coil are included. Electron temperature and bulk plasma density were estimated by Langmuir probe measurements. Electron temperatures were in the range of 3.2–6.9 and 3.1–5.0 eV for argon and deuterium plasmas, respectively, over the power and pressure range employed. The electron temperature was nearly independent of power, and increased with decreasing gas pressure in both argon and deuterium plasmas. These results are similar to other studies in inductively coupled plasmas.[13–15]

Using Laframboise's theory[16] to analyze the Langmuir probe data, it was found that plasma density was in the range of $1.4\times10^{11}-3.2\times10^{12}$ cm^{-3} and $2.9\times10^{10}-3.0\times10^{11}$ cm^{-3} in argon and deuterium plasmas, respectively, over the power and pressure range applied in this work. Bulk plasma densities increased both with power and pressure in both argon and deuterium plasmas. This behavior also agrees with other studies in inductively coupled plasmas.[13–15] Anderson *et al.*[17] measured the plasma density in deuterium and argon plasmas in a capacitively coupled discharge and they also found a higher plasma density in argon plasma.

Ion fluxes measured with a 10 μm diam hole (no plasma disturbance) allow one to estimate the ion density at the sheath edge over the hole using the Bohm criterion. The plasma density at the sheath edge over the hole was in the range of $2.2\times10^{10}-3.2\times10^{11}$ cm^{-3} and $9.7\times10^{9}-6.4\times10^{10}$ cm^{-3} for argon and deuterium plasmas, respectively. The plasma density at the sheath edge increased with plasma power as in the case of bulk plasma density. However, it decreased with increasing gas pressure. As gas pressure increases, the electron temperature decreases. This lowers the Bohm velocity of ions. Also, higher pressures result in stronger ion density gradients. Both effects tend to lower the ion flux out of the plasma. Knowing the electron temperature and plasma density at the sheath edge, the Debye length λ_D at the sheath edge was calculated. At lower pressures, when the mean free path is much greater than the sheath thickness, the sheath thickness (l) can then be estimated from $l \approx 1.1\lambda_D(eV_{sh}/kT_e)^{3/4}$, where V_{sh} is the sheath potential.[18]

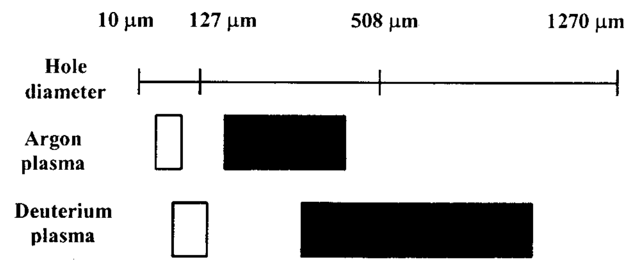

FIG. 4. Ranges of Debye length (blank rectangles), sheath thickness (black rectangles), and diameter of the holes used in this work.

Figure 4 shows the range of Debye length at the sheath edge, sheath thickness, and diameter of holes used in this work. For the calculation of the sheath thickness, the measured mean ion energy from the ion energy distribution was taken as the sheath potential. Over the power and pressure conditions employed in this study, the Debye length at the sheath edge and the sheath thickness range from 35 to 90 and from 150 to 400 μm, respectively, for argon plasmas, and from 60 to 140 and 310 to 860 μm, respectively, for deuterium plasmas. Thus, 10 μm, 508 μm, and 1270 μm diam holes represent cases where the hole diameter is much smaller than, comparable to, and larger than the sheath thickness, respectively. Two holes having the same diameter of 127 μm, but with different axial thickness (25.4 and 254 μm) were also used to investigate the effect of hole aspect ratio.

B. Current attenuation inside the ion analyzer

Ions traveling between the hole and the collecting electrodes of the ion analyzer can suffer ion–neutral collisions, potentially altering the energy and/or direction of the ions. The "effective" pressure inside the ion analyzer can be treated as the sum of a static pressure due to the gas conductance of the ion analyzer and a localized effusion pressure due to the neutrals effusing through the hole.

Many investigators[4–7,12] have placed the ion analyzer in a chamber which is differentially pumped usually to below 10^{-5} Torr. If the gas load (from the plasma source) into the analyzer is sufficiently small, and/or the gas conductance of the ion analyzer is sufficiently high, the pressure inside the ion analyzer may be low enough to neglect ion–neutral collisions. In the experimental system used in this study, although the chamber pressure in which the analyzer was housed was routinely less than 10^{-5} Torr, it is not safe to neglect the static pressure inside the analyzer. This is due to the large holes (causing a potentially high gas load) and the finite gas conductance of the analyzer.

The static pressure was determined by equating the hole throughput to the throughput of the ion analyzer. The influence of the localized effusion pressure was treated on the basis of the work of Coburn and Kay.[19] Knowing the neutral density due to the static pressure and the localized effusion

Downloaded 31 May 2002 to 129.7.12.23. Redistribution subject to AIP license or copyright, see http://ojps.aip.org/japo/japcr.jsp

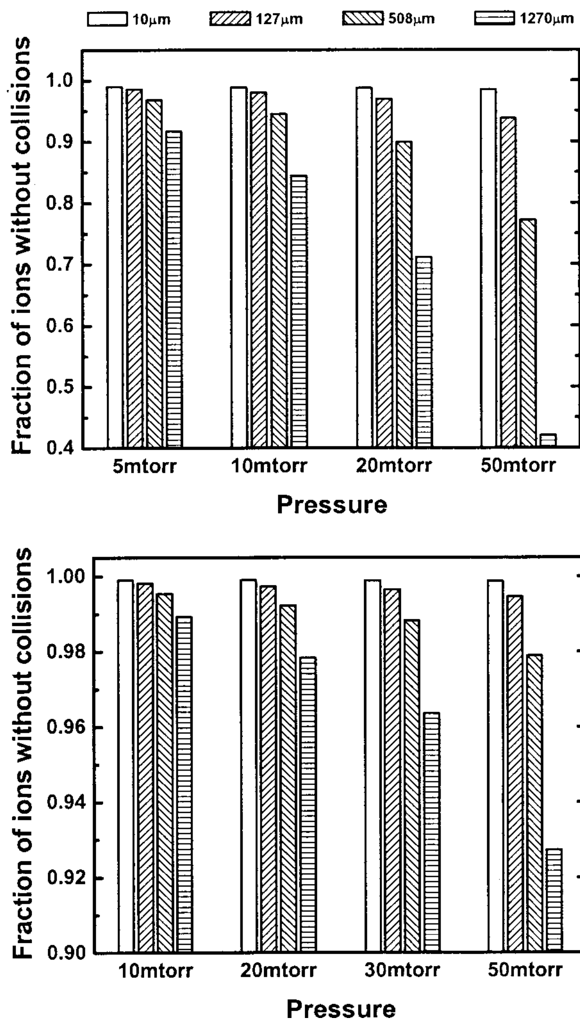

FIG. 5. Fraction of ions reaching collecting electrode along centerline without collisions with neutrals in the ion analyzer as a function of hole diameter and pressure in argon (top) and deuterium (bottom) plasmas.

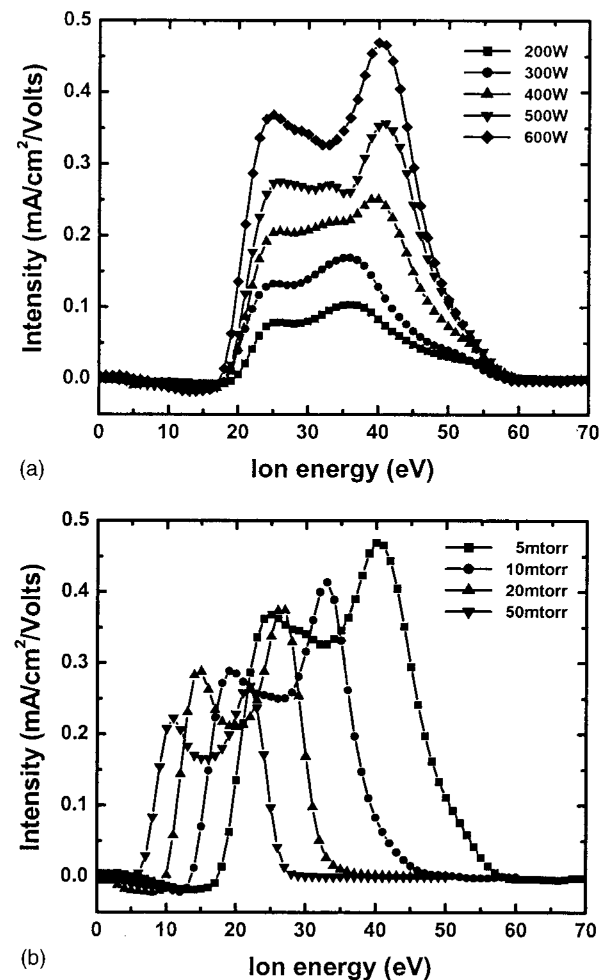

FIG. 6. Energy distributions of ions through a 10 μm diam hole for argon plasmas: (a) 5 mTorr pressure and (b) 600 W power.

pressure, the fraction of ions that reach the collecting electrode of the ion analyzer without collisions was obtained as a function of hole radius and pressure in the plasma region.

Figure 5 shows the fraction of ions reaching the collecting electrode along the center line without collisions in argon and deuterium plasmas, respectively. For this calculation, the pressure in the housing chamber was 1×10^{-5} Torr and the gas temperature was assumed to be 300 K. As expected, the fraction of ions without collisions decreases with increasing gas pressure and hole diameter. It can be seen that more than 99% of ions could reach the collecting electrode without collisions when the hole diameter is less than 10 μm. However, when the hole diameter becomes 1270 μm, ion–neutral collisions are not negligible any more, resulting in fractions of ions experiencing collisions as high as 57% and 7% in argon and deuterium plasmas, respectively. This current attenuation effect was corrected in the reported ion flux measurements at each hole size and pressure condition.

C. Ion energy distributions

Figures 6 and 7 show the energy distributions of ions through a 10 μm diam hole (no plasma disturbance) for argon and deuterium plasmas, respectively. One observes two peaks in argon and four peaks in deuterium, respectively. The structure of the ion energy distribution (IED) suggests that the plasma potential is modulated. This is due to stray capacitive coupling from the unshielded coil and the beam acceleration electrode (Fig. 2) to the plasma. The amount of capacitive coupling from the beam acceleration electrode was minimized for each experiment by tuning the capacitor of the circuit connected to the beam acceleration electrode shown in Fig. 2. The stray capacitive coupling resulted in a rf biased sheath over the grounded electrode with the hole.

The shape of the ion energy distribution in a rf sheath depends critically on the product of the ion transit time τ_i and the angular frequency of the applied field $(\omega=1/T)$.[20,21] When $\omega\tau_i\ll1$, ions cross the sheath in a short time compared to the field oscillations. Under this condition, the ion energy will depend on the phase of the rf cycle when the ion enters the sheath. Thus, ion energy distributions are double peaked (for a single ion) with the maximum and minimum energies corresponding to ions crossing the sheath during the maximum and minimum sheath potential, respectively. On the other hand, when $\omega\tau_i\gg1$, ions experience many field oscillations while crossing the sheath. The ion energy will then depend on the average sheath potential, resulting in a single

Downloaded 31 May 2002 to 129.7.12.23. Redistribution subject to AIP license or copyright, see http://ojps.aip.org/japo/japcr.jsp

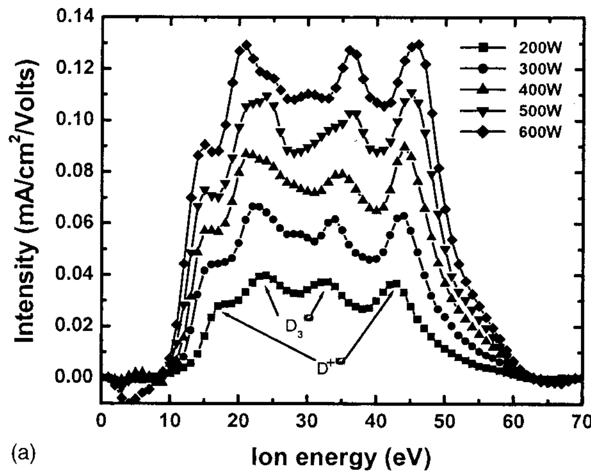

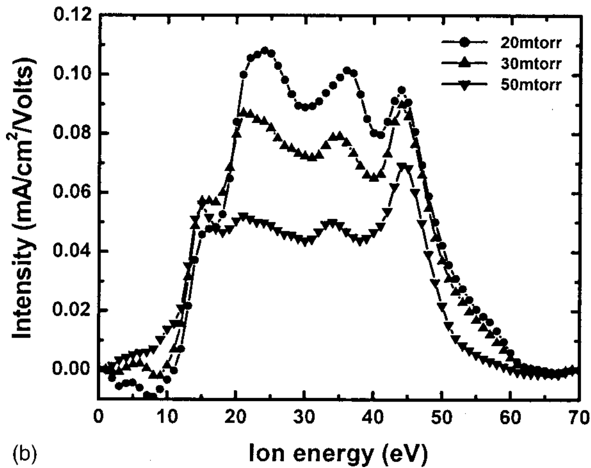

FIG. 7. Energy distributions of ions through a 10 μm diam hole for deuterium plasmas: (a) 30 mTorr pressure and (b) 400 W power.

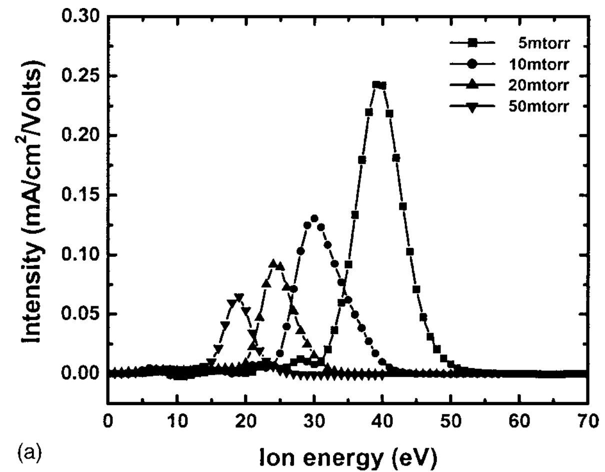

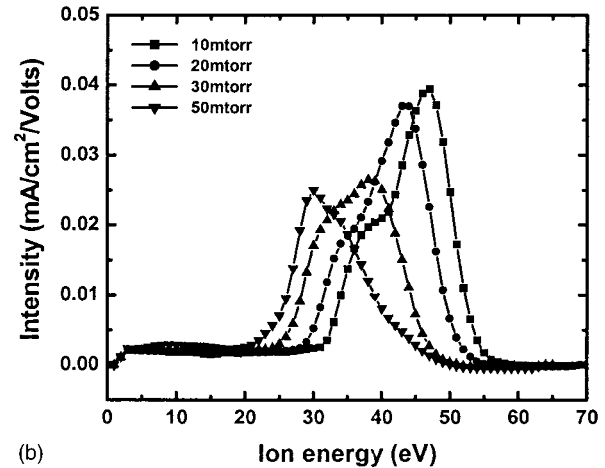

FIG. 8. Energy distributions of ions through a 1270 μm diam hole: (a) argon plasmas at 600 W and (b) deuterium plasmas at 600 W.

peak in the ion energy distributions. The ion transit time can be estimated as the inverse of the ion plasma frequency (ω_{pi}) based on the plasma density at the sheath edge,[21] $\tau_i = 1/\omega_{pi}$, where $\omega_{pi} = (e^2 n_{is}/\varepsilon_0 m_i)^{1/2}$. Using the angular frequency of $(2\pi) \times (13.56\ \mathrm{MHz}) = 8.52\times 10^7\ \mathrm{s}^{-1}$, one finds that $\omega\tau_i$ is about 0.7–2.7 for Ar^+ ions, and 0.4–0.9 and 0.6–1.6 for D^+ and D_3^+ ions (see below), respectively, over the range of power and pressure applied in this study. Ulacia and McVittie[22] pointed out that the modulation of ion energy is still apparent even when the ion transit time is about five rf periods. Thus, the energy of ions impinging on the 10 μm diam hole should be modulated.

It is known[23,24] that the energy separation ΔE of a pair of peaks (corresponding to an ion) in the IED is inversely proportional to the square root of the ion mass. Thus, for two ions with masses m_i and m_o one has, $\Delta E_o/\Delta E_i = (m_i/m_o)^{1/2}$, where subscripts i and o correspond to the inner and outer pairs of peaks of the IED, respectively. The measured energy separations of the inner and outer peak pairs of the IED for deuterium (Fig. 7, top), supported the hypothesis that D^+ and D_3^+ are the dominant ions in the plasma, i.e., the energy separation ratio predicted for the D^+/D_3^+ pair was closest to the measured energy separation, when compared to the other possible ion pairs. However, the presence of D_2^+ in the plasma cannot be ruled out since the peaks of the IED are not sharp, and species identification based on ΔE alone does not suffice.

At a constant pressure (Figs. 6, top and 7, top), the peak, minimum, and maximum ion energy are nearly constant as power is varied in both argon and deuterium plasmas. This behavior is consistent with other studies in argon or other discharges.[4–7,9] It is a characteristic of ion energy distributions in inductively coupled plasmas. In these plasmas, plasma power controls ion flux, not ion energy.

In an argon plasma, the peak, minimum and maximum ion energy decrease as pressure was increased at constant power (Fig. 6, bottom). It is expected that ions will experience more collisions with increasing pressure, resulting in lower ion energy. In a deuterium plasma, however, ions impinging on the 10 μm diam hole have a nearly constant peak, minimum, and maximum energy as pressure is varied at constant power (Fig. 7, bottom). In deuterium plasmas, the collision cross section of ions with neutrals is much lower than that in argon plasmas, making ion flow (through the sheath and through the analyzer behind the 10 μm hole) collisionless over the pressure range applied in this work.

Figure 8 shows the energy distributions of ions impinging on a 1270 μm diam hole at a given power. In an argon plasma (Fig. 8, top), the peak, minimum, and maximum ion energy decrease as pressure is increased, due to more ion–

Downloaded 31 May 2002 to 129.7.12.23. Redistribution subject to AIP license or copyright, see http://ojps.aip.org/japo/japcr.jsp

neutral collisions with pressure. In a deuterium plasma [Fig. 8 (bottom)], the peak, minimum, and maximum ion energy also decrease as pressure is increased. This is in contrast to the case of the 10 μm diam hole (Fig. 7, bottom). This is due to ion–neutral collisions mainly in the space between the hole and the collecting electrodes of the ion analyzer. With a large diameter hole, the gas load effusing from the plasma into the analyzer body (Fig. 2) establishes a high enough pressure inside the analyzer that even deuterium ions can suffer a collision.

The striking difference in the ion energy distributions between Figs. 6 and 8, however, is that the 10 μm diam hole produces two or four peaks in argon or deuterium plasmas, respectively, while the 1270 μm diam hole results in a single peak in argon and a single peak with a shoulder in deuterium plasmas. This implies plasma leakage into the 1270 μm diam hole. Note that the 1270 μm diam hole is larger than the sheath thickness (see Fig. 4). If plasma penetrates into the hole, ions escaping from the plasma will be hardly affected by the sheath between the plasma and the solid wall, and will arrive at the detecting electrode experiencing the average plasma potential, because their transit time is correspondingly larger (see Fig. 1). Thus, the ion energy distributions will have a single peak. The shoulder of the peaks in the deuterium plasmas may be a consequence of the fact that deuterium ions are quite light and some residual modulation of their energy still remains.

The IED of ions extracted from a 508 μm diam hole (Fig. 9) appears to be in-between the distributions measured with the 10 μm and 1270 μm diam holes. Since the size of the 508 μm diam hole is comparable to the sheath thickness (Fig. 4), plasma will penetrate the hole partly, as depicted in Fig. 1, bottom.

The mean ion energy was obtained by integrating the ion energy distribution function. It was found that the mean ion energies are nearly constant with power in all cases in both argon and deuterium plasmas. This is consistent with other studies in inductively coupled plasmas in which plasma power only weakly affects the mean ion energy.[4,24] This is in contrast to capacitively coupled plasmas, in which the mean ion energy with the rf peak-to-peak voltage.

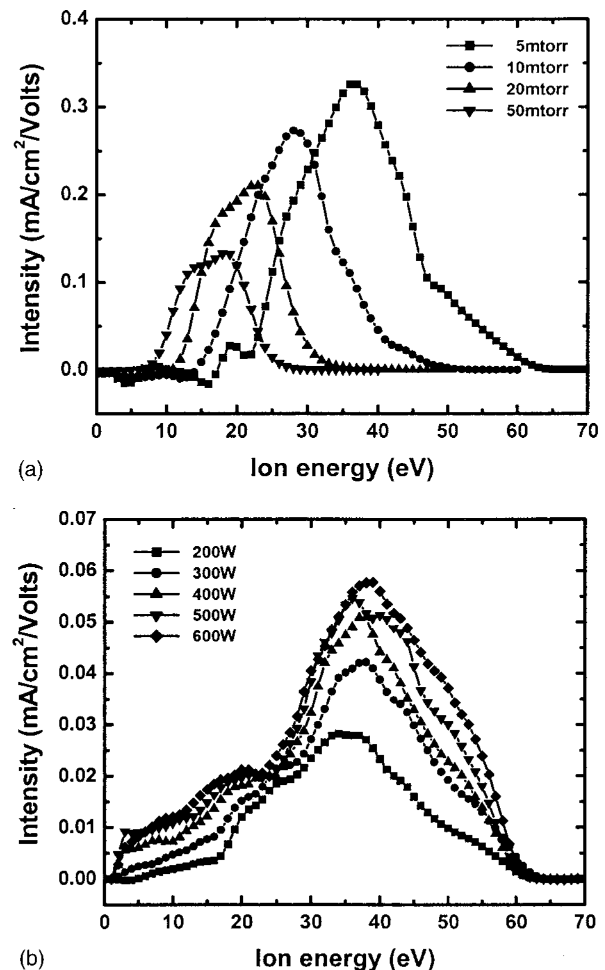

FIG. 9. Energy distributions of ions through a 508 μm diam hole: (a) argon plasmas at 400 W and (b) deuterium plasmas at 30 mTorr.

D. Ion increases angular distributions

Ion angular distributions were measured by the sectioned ion analyzer (Fig. 3). The area of each collecting electrode varies by more than a factor of 70 as one moves from the smaller circular electrode at the center to the largest annular electrode at the edge of the ion detector. It was necessary, therefore, to divide the raw signals from each electrode by the electrode area in order to obtain measurements of ion flux versus angle.

Figure 10 shows that the angular distributions of ions through a 10 μm diam hole in argon and deuterium plasmas are nearly Gaussian peaking at zero angle from the surface normal. Since the sheath thickness is much larger than 10 μm, the plasma is not perturbed by the presence of the hole (see Fig. 1, top). Many experimental and theoretical studies[25,26] suggest that the ion angular distribution is approximately Gaussian when the ion trajectories are not perturbed by fringing electric fields around the hole. For Gaussian distributions, the ion angular distribution function $f(\theta)$ is given by[26] $f(\theta)=C_N\exp(-\beta\theta^2)$, where C_N is a normalization constant, θ is the incidence angle measured from the surface normal, and $\beta=eV_{sh}/kT_+$ is the ratio of the directed energy gained in the sheath (equal to the sheath potential, V_{sh}, if $V_{sh}\gg T_e$) to the ion temperature T_+. Parameter β determines the full width at half maximum (FWHM) of the ion angular distribution $\Delta\theta_{FWHM}=2\sqrt{\ln 2/\beta}$. At given pressure, the FWHM was found to increase with power in both argon and deuterium plasmas. In argon plasmas, the FWHM increased as pressure was increased due to collisions with neutrals. However, the FWHM remained nearly constant as pressure was varied in deuterium plasmas because of the much lower collisionality of these plasmas.

When plasma leaks into the hole, the ion angular distributions are not Gaussian any more. Figures 11 and 12 show the angular distributions of ions impinging on 508 and 1270 μm diam holes, respectively. The ion angular distributions are very broad because of plasma leakage into the holes. When the hole diameter (508 μm) is comparable to the sheath thickness, the ion angular distributions become a bit

Downloaded 31 May 2002 to 129.7.12.23. Redistribution subject to AIP license or copyright, see http://ojps.aip.org/japo/japcr.jsp

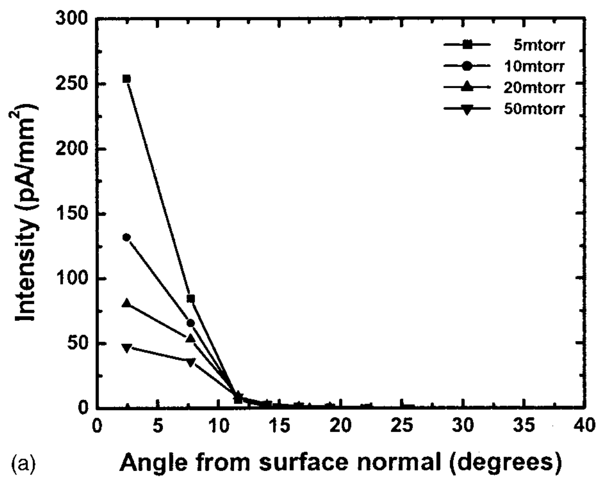

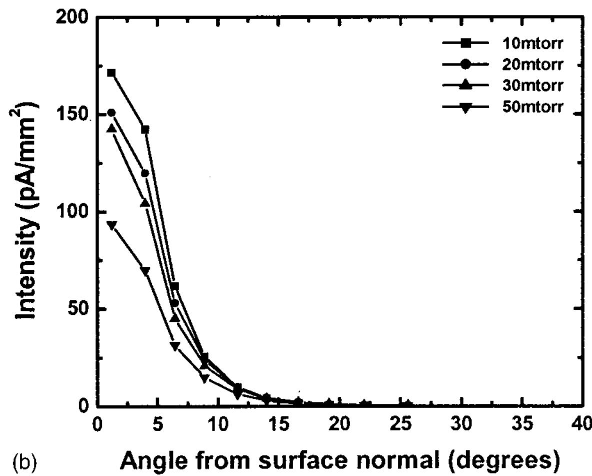

FIG. 10. Angular distributions of ions through a 10 μm diam hole: (a) argon plasmas at 600 W and (b) deuterium plasmas at 600 W.

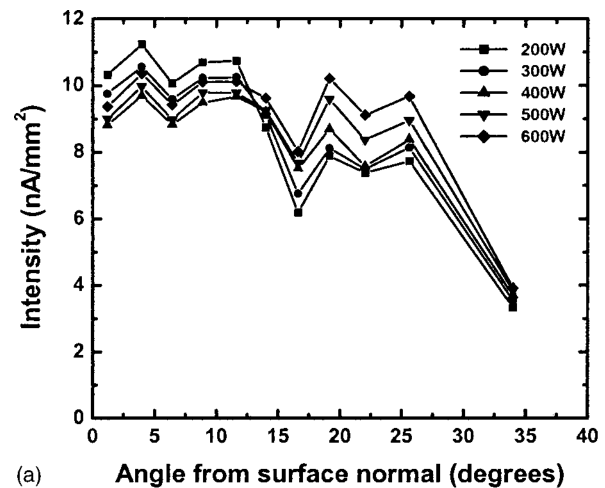

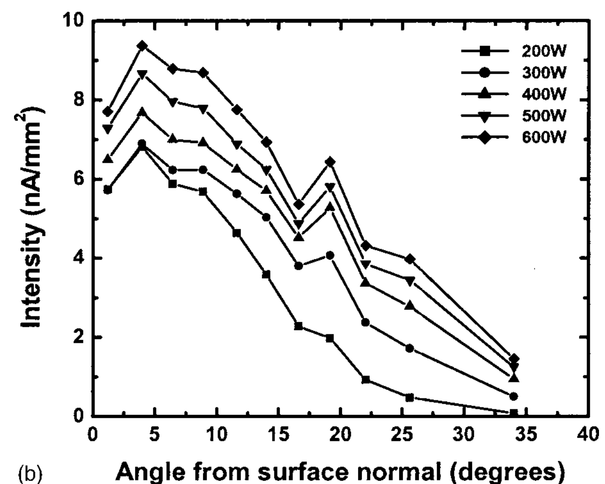

FIG. 11. Angular distributions of ions through a 508 μm diam hole: (a) argon plasmas at 20 mTorr and (b) deuterium plasmas at 50 mTorr.

more isotropic as power is increased at a given pressure in both argon and deuterium plasmas (Fig. 11). In this case, the plasma–sheath boundary is located inside the hole (Fig. 1, bottom). The plasma meniscus gets closer to the bottom of the hole as power is increased (thinner sheath) resulting in more isotropic distributions of ion angles. When the hole diameter (1208 μm) is larger than the sheath thickness (Fig. 12), the ion angular distributions are fairly isotropic up to 30° from the surface normal over the power and pressure range used. In this case, the ion angular distribution shapes are nearly constant with power and pressure in both argon and deuterium plasmas, implying that plasma fully penetrates into the hole.

Hole aspect ratio also affects the ion angular distribution. Figure 13 shows the angular distributions of ions impinging on 127 μm diam holes with 24.5 and 245 μm thickness, respectively, in deuterium plasmas. The intensity was normalized by the maximum intensity for each power for better comparison. When the hole aspect ratio increases (open symbols), the ion angular distribution drops to zero faster, because ions in the wings of the distribution collide with the sidewalls of the hole and are neutralized. The possibility of ions striking the sidewalls of the higher aspect ratio hole can also be inferred from the ion flux (not shown). It was found that the total ion flux measured with the higher aspect ratio (thicker) hole was smaller compared to that measured with the lower aspect ratio hole.

The desired angular spread of ions extracted from a plasma depends on the application. For example, anisotropic etching requires a collimated beam, while coating or cleaning of the sidewalls of surface features is facilitated with divergent beams. Therefore, it is very useful to know the degree of ion beam divergence (cone of ion angles) at a given plasma condition. Figure 14 shows the angle of the cone into which 50% of ions are contained as a function of the ratio of the hole diameter to the sheath thickness, for deuterium plasmas. A similar plot was obtained for argon plasmas. In this plot, the measured ion angles were taken to be limited by the ion analyzer when the ion current at the maximum angle than can be captured by the ion analyzer (34°) was larger than 30% of the maximum current at a given experimental condition. According to this criterion, filled symbols or open symbols in Fig. 14 represent ion angles limited or not limited by the ion analyzer, respectively.

When the ratio of the hole diameter to the sheath thickness is much less than unity (0.01–0.03), the angle is saturated at about 4°. In this regime, the hole diameter is much smaller than the sheath thickness and the plasma–sheath meniscus is planar (see Fig. 1, top). Thus, variation of the hole

Downloaded 31 May 2002 to 129.7.12.23. Redistribution subject to AIP license or copyright, see http://ojps.aip.org/japo/japcr.jsp

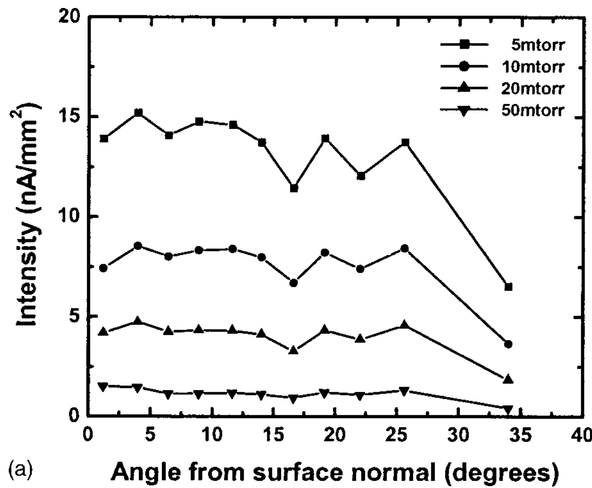

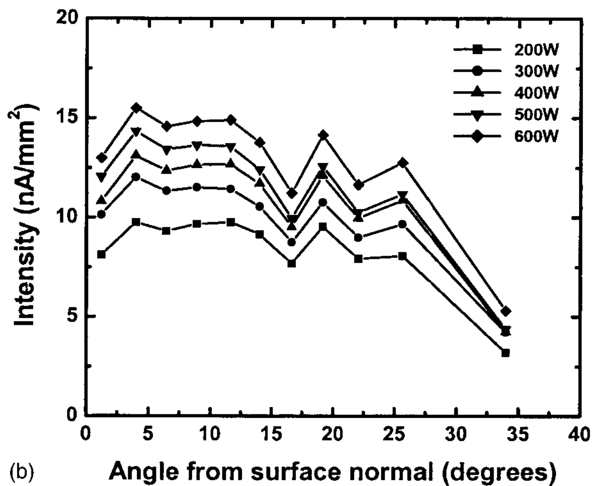

FIG. 12. Angular distributions of ions through a 1270 μm diam hole: (a) argon plasmas at 200 W and (b) deuterium plasmas at 20 mTorr.

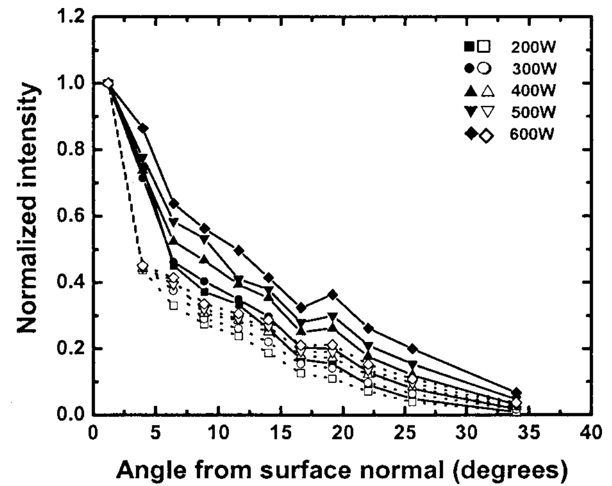

FIG. 13. Angular distributions of ions through a 127 μm diam hole in deuterium plasmas at 10 mTorr pressure. Filled and open symbols correspond to 25.4 and 254 μm thickness of the hole, respectively. Intensities were normalized with respect to maximum intensity at given power.

diameter does not affect significantly the cone of ion angles. When the ratio of the hole diameter to the sheath thickness increases (0.2–2), the cone of ion angles increases dramatically. In this regime, the plasma starts bulging into the hole. Therefore, ions spread and the cone of ion angles increases. When the ratio of the hole diameter to the sheath thickness increases further (>3), the cone of ion angles saturates at about 16°. This value is limited by the geometry of the ion analyzer used in this work. Nevertheless, the ion angles are still expected to saturate (at a larger angle) for large hole diameter to sheath thickness ratios. In this regime, the plasma would leak completely out of the hole (see Fig. 1, middle). Therefore, the variation of the hole diameter should not affect significantly the cone of ion angles.

IV. CONCLUSIONS

Plasma molding over surface topography was investigated by measuring the energy and angular distribution of ions extracted from a hole in contact with a high density plasma. Interaction of a plasma with a single hole was thought to be a well-defined experiment to study plasma–grid interaction. Holes with 10, 508, or 1270 μm in diameter were used to represent the cases of hole diameter much less than, comparable to, or larger than the sheath thickness, respectively. Holes having the same diameter of 127 μm, but with different thickness (25.4 and 254 μm) were also used to study the effect of the hole aspect ratio.

The ion energy distribution showed different behavior according to the hole diameter. When the hole diameter (10 μm) was much less than the sheath thickness, the ion energy distribution had multiple peaks: two peaks in argon (due to one ion species, Ar^+) and four peaks in deuterium (due to two ion species, D^+ and D_3^+). The ion energy was modulated, because the ion transit time through the sheath was smaller than or comparable to the rf period. The peak, minimum, and maximum ion energy were nearly constant as power was varied in both argon and deuterium plasmas. This is because in inductively coupled plasmas, plasma power controls ion flux, not ion energy. The peak, minimum, and maximum ion energy decreased with increasing pressure in

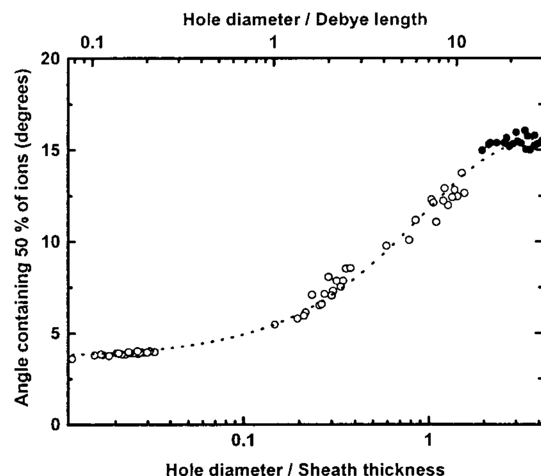

FIG. 14. Angle of cone into which 50% of ions are contained as a function of the ratio of the hole diameter to the sheath thickness for deuterium plasmas. Filled and open symbols represent ion angles limited or not limited by the ion analyzer, respectively.

Downloaded 31 May 2002 to 129.7.12.23. Redistribution subject to AIP license or copyright, see http://ojps.aip.org/japo/japcr.jsp

argon plasmas since ions experienced more collisions with neutrals. In deuterium plasmas, however, the collision cross section of ions with neutrals is much lower. As a result, the peak, minimum, and maximum ion energy were nearly independent of pressure.

When the hole diameter (1270 μm) was larger than the sheath thickness, the plasma penetrated into the hole. Ions then experienced the average sheath potential, resulting in ion energy distributions with a single peak in argon plasmas and a single peak with a shoulder in deuterium plasmas. The peak, minimum, and maximum ion energy decreased with increasing pressure even in deuterium plasmas due to ion–neutral collisions inside the ion analyzer. When the hole diameter (508 μm) was comparable to the sheath thickness, the ion angular distributions (IEDs) and IADs were in-between those for the 10 and 1270 μm diam cases.

The IAD was also greatly affected by the hole diameter. When the hole diameter (10 μm) was much less than the sheath thickness, the IAD had a Gaussian shape peaked at zero angle from the surface normal in both argon and deuterium plasmas. The FWHM increased with increasing power in both argon and deuterium plasmas. The FWHM also increased with pressure in argon plasmas due to more ion–neutral collisions. In deuterium plasmas, however, the FWHM was weakly affected by pressure since ion flow was nearly collisionless.

When the hole diameter (508 μm) was comparable to the sheath thickness, the ion angular distribution was not Gaussian. The ion angular distribution became a bit more isotropic as power was increased in both argon and deuterium plasmas. In this case, the plasma–sheath meniscus got closer to the bottom of the hole with increasing power (thinner sheath), resulting in more isotropic distributions of ion angles. When the hole diameter (1270 μm) was larger than the sheath thickness, the ion angular distribution in both argon and deuterium plasmas was fairly isotropic up to 30° from the surface normal. The shape of the ion angular distribution was nearly constant with power and pressure, implying that plasma leaked completely into the hole.

The ion angular distribution measured from holes having the same diameter of 127 μm but different thickness (25.4 and 254 μm) showed that the IAD was also affected by the hole aspect ratio. When the hole aspect ratio increased, the IAD was narrower and dropped to zero faster. In this case, ions in the wings of the distribution collided with the sidewalls of the hole and were neutralized.

The angle defining the cone into which 50% of ions are contained was saturated when the ratio of the hole diameter to the sheath thickness (d/l) was much smaller than or much larger than unity in both argon and deuterium plasmas. When $d/l \ll 1$, the plasma–sheath meniscus would be planar, while when $d/l \gg 1$, the plasma would leak completely out of the hole. When $d/l \sim 1$, the cone of ion angles increased with the ratio of the hole diameter to the sheath thickness. In this regime, the plasma would start bulging into the hole, resulting in progressively higher spread of ion angles. The largest angle was limited by the geometry of the ion analyzer to about 16°.

ACKNOWLEDGMENTS

Financial support for this work was provided by Sandia National Laboratories (SNL) and the National Science Foundation. Many thanks to Dr. J. Woodworth of SNL for help with the ion detector, and to Dr. L. Chen of Chen Laboratories for help with the plasma source.

[1] H. R. Kaufman and R. S. Robinson, in *Handbook of Plasma Processing Technology*, edited by S. M. Rossnagel, J. J. Cuomo, and W. D. Westwood, (Noyes, NJ, 1990).
[2] L. Chen and Q. Yang, Proc.-Electrochem. Soc. **96-12**, 332 (1996); L. Chen, A. Sekiguchi, and D. Podlesnik, Mater. Res. Soc. Symp. Proc. **279**, 803 (1993).
[3] S. Panda, D. J. Economou, and L. Chen, J. Vac. Sci. Technol. A **19**, 398 (2001).
[4] J. R. Woodworth, M. E. Riley, D. C. Meister, B. P. Aragon, M. S. Le, and H. H. Sawin, J. Appl. Phys. **80**, 1304 (1996).
[5] J. R. Woodworth, M. E. Riley, P. A. Miller, G. A. Hebner, and T. W. Hamilton, J. Appl. Phys. **81**, 5950 (1997).
[6] J. R. Woodworth, M. E. Riley, P. A. Miller, C. A. Nichols, and T. W. Hamilton, J. Vac. Sci. Technol. A **15**, 3015 (1997).
[7] C. A. Nichols, J. R. Woodworth, and T. W. Hamilton, J. Vac. Sci. Technol. A **16**, 3389 (1998).
[8] S. G. Ingram and N. St. J. Braithwaite, J. Phys. D **21**, 1496 (1988).
[9] J. Hopwood, Appl. Phys. Lett. **62**, 940 (1993).
[10] P. A. Talyor, J. Vac. Sci. Technol. A **6**, 2583 (1988).
[11] Y. Sakai and I. Katsumata, Jpn. J. Appl. Phys., Part 1 **24**, 337 (1985).
[12] J. Liu, G. L. Huppert, and H. H. Sawin, J. Appl. Phys. **68**, 3916 (1990).
[13] A. Schwabedissen, E. C. Benck, and J. R. Roberts, Phys. Rev. E **55**, 3450 (1997).
[14] J. Hopwood, C. R. Guarnieri, S. J. Whitehair, and J. J. Cuomo, J. Vac. Sci. Technol. A **11**, 152 (1993).
[15] P. A. Miller, G. A. Hebner, K. E. Greenberg, P. D. Pochan, and B. P. Aragon, J. Res. Natl. Inst. Stand. Technol. **100**, 427 (1995).
[16] J. G. Laframboise, *University of Toronto Institute Aerospace Studies Report* No. 100, 1966.
[17] C. A. Anderson, M. B. Hopkins, and W. G. Graham, Rev. Sci. Instrum. **61**, 448 (1990).
[18] F. F. Chen, *Introduction to Plasma Physics and Controlled Fusion* (Plenum Press, New York, 1984).
[19] J. W. Coburn and E. Kay, J. Vac. Sci. Technol. **8**, 738 (1971).
[20] T. Panagopoulos and D. J. Economou, J. Appl. Phys. **85**, 3435 (1999).
[21] P. A. Miller and M. E. Riley, J. Appl. Phys. **82**, 3689 (1997).
[22] J. I. Ulacia F. and J. P. McVittie, J. Appl. Phys. **65**, 1484 (1989).
[23] Y. Okamoto and H. Tamagawa, J. Phys. Soc. Jpn. **29**, 187 (1970).
[24] E. A. Edelberg, A. Perry, N. Benjamin, and E. S. Aydil, J. Vac. Sci. Technol. A **17**, 506 (1999).
[25] E. S. Aydil, B. O. M. Quiniou, J. T. C. Lee, J. A. Gregus, and R. A. Gottscho, Mater. Sci. Semicond. Process. **1**, 75 (1998).
[26] R. A. Gottscho, J. Vac. Sci. Technol. B **11**, 1884 (1993).

Downloaded 31 May 2002 to 129.7.12.23. Redistribution subject to AIP license or copyright, see http://ojps.aip.org/japo/japcr.jsp